Enabling electron conduction in anisotropic hole transport materials for superior optical properties in organic light emitting diodes

Markus Schmid,[1] Thomas Morgenstern,[1] and Wolfgang Brütting[1, a)]

Institute of Physics, University of Augsburg, 86135 Augsburg,

Germany

(Dated: 11 July 2018)

Alignment of the emitter molecules in organic light emitting diodes (OLEDs) has attracted growing attention in recent years as it can significantly increase the device efficiency. There is continuous progress in tailoring dyes towards a higher degree of horizontal orientation with respect to the substrate plane. While most of the studies focus on the emitting layer, this report will discuss orientation in the transport layers of the diode. Alignment of the molecules within a neat film can lead to optical anisotropy. From a theoretical point of view it was shown, that birefringence can increase OLED efficiency. In this study we demonstrate this effect for actual OLED materials. We will present a strategy to modify the charge transport in a birefringent hole conductor. Doping with cesium carbonate (Cs_2CO_3) resulted in good electron conduction in the usually hole transporting material. Efficient devices were realized utilizing the doped material as electron transport layer. Optical simulations confirm the benefit for OLEDs through superior optical properties of the modified transport layer.

Keywords: molecular orientation, optical anisotropy, doping, optical simulation

---

[a)]Electronic mail: bruetting@physik.uni-augsburg.de

Organic light emitting diodes (OLEDs) are promising light-sources for display and general lighting technologies because of their outstanding features like large area, low thickness and weight as well as their potential flexibility[1–3]. One of the main issues is a further increase of the device efficiency[3]. A promising way to realize a better performance is taking advantage of orientation within amorphous layers. Especially emitter molecules that are oriented parallel with respect to the substrate plane have attracted growing attention recently[4–6]. In this study we focus on effects in the transport layers of an OLED caused by a predominant molecular alignment in the film. Due to the fact that both transition dipole moment and polarizability are larger along the long axis of molecules, horizontal orientation results in a larger refractive index (n_o) parallel to the substrate than perpendicular to this plane (n_e)[7,8]. Simulations in a generic device structure show that this so called negative birefringence can slightly increase the device efficiency[9]. In the following, we will first discuss this effect for actual OLED materials. Afterwards we will present a strategy to modify the transport properties of a birefringent hole conducting material in order to employ it as an electron transport layer.

The OLED efficiency is described by the external quantum effiency (EQE) η_EQE that can be written in four factors:

$$\eta_\mathrm{EQE} = \gamma \times \eta_\mathrm{S/T} \times q_\mathrm{eff} \times \eta_\mathrm{out}. \tag{1}$$

Therein γ, $\eta_\mathrm{S/T}$, q_eff and η_out describe the charge carrier balance, the singlet-triplet factor, the effective radiative quantum efficiency and the outcoupling efficiency, respectively[10]. The factors q_eff and η_out are both dependent on the OLED microcavity and thus influenced by the optical constants[3]. Calculations in the work of Callens *et. al.*[9] show that negative birefringence of the material next to the reflective back-electrode can increase the factor η_out resulting in a higher EQE for bottom-emitting OLEDs. In the typical device structure with a reflective cathode, this means that negatively birefringent electron transport materials can increase the device efficiency. However, we are not aware of many commercially available materials, apart from 4,6-Bis(3,5-di-3-pyridinylphenyl)-2-methylpyrimidine (B3PyMPM) and some similar derivatives, that show a significant anisotropy of their optical constants[11] and are suitable for electron transport[12]. By contrast, Tris(4-carbazoyl-9-ylphenyl)amine (TCTA) a hole transport material[13–15] shows birefringence. Apart from hole conduction TCTA is also used for electron confinement[16] and exciton-confinement[16–18]. Further down in this work we will show that it can be turned to electron conducting by doping with Cs_2CO_3. Figure 1
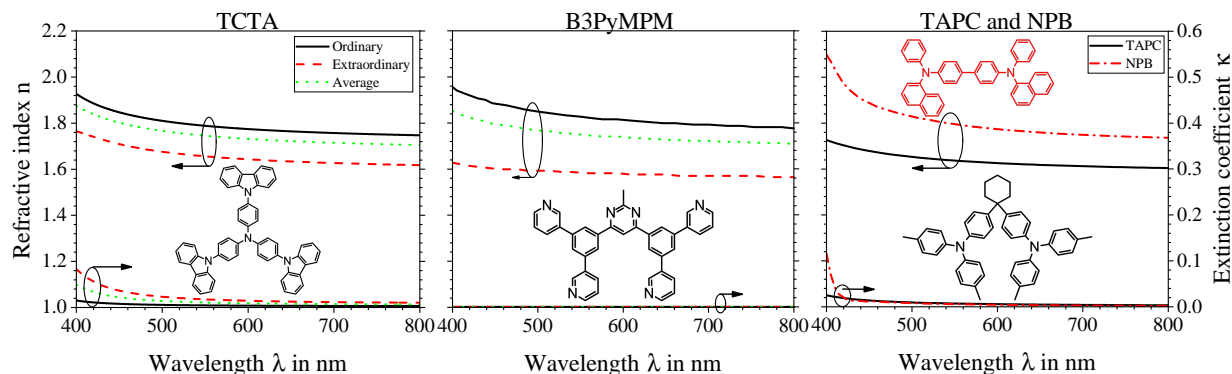
FIG. 1. Optical constants of TCTA, B3PyMPM, TAPC and NPB. The refractive index of B3PyMPM was taken from reference[11]. TCTA, TAPC and NPB were investigated with variable angle spectroscopic ellipsometry in our group. The ellipsometric data and fits are shown in the supporting information.

shows the refractive indices and the chemical structures of B3PyMPM, TCTA and the optically isotropic 4,4-Cyclohexylidenebis[N,N-bis(4-methylphenyl)benzenamine] (TAPC) and N,N-Bis(naphthalen-1-yl)-N,N-bis(phenyl)benzidine (NPB), which were used as hole transport materials, for comparison.

In order to study a potential effect from the birefringence of the candidates we performed optical simulations on three different device structures (see table I for details). As usual in bottom emitting OLEDs the first layer of the diodes is a transparent indium tin oxide (ITO) anode. In device structure (1) the anode is followed by 1,4,5,8,9,11-Hexaazatriphenylene-hexacarbonitrile (HAT-CN) and NPB for hole injection and transport, respectively. The emission arises from the phosphorescent emitter Iridium(III)bis(2-methyldibenzo-[f,h]quino-xaline)(acetylacetonate) (Ir(mdq)$_2$(acac)) doped in the hole conductor NPB, which is a typical host for this Iridium complex[19–21]. In order to avoid the drift of holes through the complete device, a hole blocking layer of 1,3-Bis[2-(4-tert-butylphenyl)-1,3,4-oxadiazo-5-yl]-benzene (OXD-7) is added in front of the birefringent electron transporting layers B3PyMPM and TCTA. In device structure (2) the light emission arises from the green phosphorescent emitter Bis[2-(2-pyridinyl-N)phenyl-C](acetylacetonato)iridium(III) (Ir(ppy)$_2$(acac)) doped in 1,3-Bis(N-carbazolyl)benzene (mCP). The hole injection and conduction layers are not changed in comparison to diode (1), but an additional electron blocking layer of pure TCTA is required. OXD-7 again serves as hole blocking layer and is followed by TCTA for elec-

tron conduction. A 100 nm thick layer of aluminum completes both OLED stacks. Device structure (3) was inspired by the publication of Kim *et. al.*[12]. In this work the ITO anode is directly followed by the hole conductor TAPC and the electron blocking layer TCTA. The emitter Ir(ppy)$_2$(acac) is doped in the exciplex forming co-host TCTA:B3PyMPM. B3PyMPM is also responsible for electron conduction. Finally aluminum again serves as cathode. An exceptionally high external quantum efficiency (EQE) of more than 30 % was presented using this stack layout. Note that the high EQE in the work of Kim *et. al.* was achieved in devices having a rather thin ITO layer (70 nm). However, for comparison with devices (1) and (2) we performed all simulations with $d_\mathrm{ITO} = 150$ nm. Importantly, the horizontal orientation of the dyes described by the value of $\Theta = 0.24$[20,22] and the intrinsic quantum efficiency $q = 0.7$ for Ir(mdq)$_2$(acac)[20] and $q = 0.94$ for Ir(ppy)$_2$(acac)[12] were taken into account in the calculations.

The thicknesses of the electron and hole conducting layers were varied in the simulation to optimize the OLED microcavity. At first the calculation was performed with the actual anisotropic optical constants for B3PyMPM and TCTA (black solid and red broken line in figure 1). Afterwards another optimization using average optical constants was run (green dotted line in figure 1). The average refractive index is an estimation for the optically isotropic refractive index. It is calculated via the formula

$$n_\mathrm{avg} = \sqrt{\frac{1}{3}\left(2n_\mathrm{o}^2 + n_\mathrm{e}^2\right)} \tag{2}$$

from the ordinary and extraordinary refractive indices n_o and n_e, respectively[9]. The layer thicknesses and the maximum calculated quantum efficiencies are summarized in table I. Figure 2 additionally shows the maximum possible EQE in dependence of the electron transport layer thickness at the optimum layer thickness of the hole transport material.

It is evident from these data that the simulated EQE of the device structures containing the green emitter Ir(ppy)$_2$(acac) is larger than the calculated efficiencies for the red dye Ir(mdq)$_2$(acac). The reason is the higher intrinsic quantum efficiency of Ir(ppy)$_2$(acac) ($q = 0.94$[12]) compared with Ir(mdq)$_2$(acac) ($q = 0.7$[20]). The comparison between the calculation with birefringent (closed symbols) and average optical constants (open symbols) is of greater interest. Independently of the emitter and the device structure the calculation yields a higher maximum EQE, if birefringence is taken into account compared with the simulation in which the average refractive index is assumed. The results are comparable to the calculations

Device Structure (used ETL)	n	d_{ETL} in nm	d_{HTL} in nm	$\eta_{\text{EQE,max}}$
1 (TCTA)	bir	65	38	21.7 %
1 (TCTA)	avg	67	36	21.2 %
1 (B3PyMPM)	bir	63	38	22.3 %
1 (B3PyMPM)	avg	65	36	21.4 %
2	bir	47	10	24.1 %
2	avg	51	10	23.2 %
3	bir	41	86	26.3 %
3	avg	49	82	24.4 %

TABLE I. Summary of the simulation results with birefringent and average optical constants of the anisotropic transport materials. The optimum thickness for the electron transport layer d_{ETL} and the hole transport layer d_{HTL} and the maximum possible EQE ($\eta_{\text{EQE,max}}$) is listed. Device structures are:

(1): ITO (150 nm), HAT-CN (10 nm), NPB (d_{HTL}), NPB:Ir(mdq)$_2$(acac) (10 nm), OXD-7 (10 nm), TCTA / B3PyMPM (d_{ETL}) and Al (100 nm)

(2): ITO (150 nm), HAT-CN (10 nm), NPB (d_{HTL}), TCTA (10 nm), mCP:Ir(ppy)$_2$(acac) (10 nm), OXD-7 (10 nm), TCTA (d_{ETL}) and Al (100 nm)

(3): ITO (150 nm), TAPC (d_{HTL}), TCTA (10 nm), TCTA:B3PyMPM:Ir(ppy)$_2$(acac) (30 nm), B3PyMPM (d_{ETL}) and Al (100 nm).

presented by Callens $et.$ $al.$[9] although their simulations were performed with a strongly simplified device structure and a monochromatic emitter. The effect naturally is stronger for the materials showing a greater anisotropy. Thus the relative change $\left(\frac{\eta_{\text{EQE,max,bir}}}{\eta_{\text{EQE,max,avg}}} - 1 \right)$ is bigger for B3PyMPM (8.0 and 4.2 %) than TCTA (3.7 and 2.8 %) for the green and the red dye, respectively. Additionally we expect a larger relative effect in dependence on the emitter. This is due to the different quantum efficiencies of the Iridium complexes. The application of a birefringent electron transport layer reduces the Purcell factor F of the OLED microcavity[9]. For highly efficient emitters the Purcell effect does not lead to a higher effective radiative quantum efficiency[3]. A reduction of F thus has a minor impact on the maximum EQE for the more efficient emitter. The relative change is indeed larger
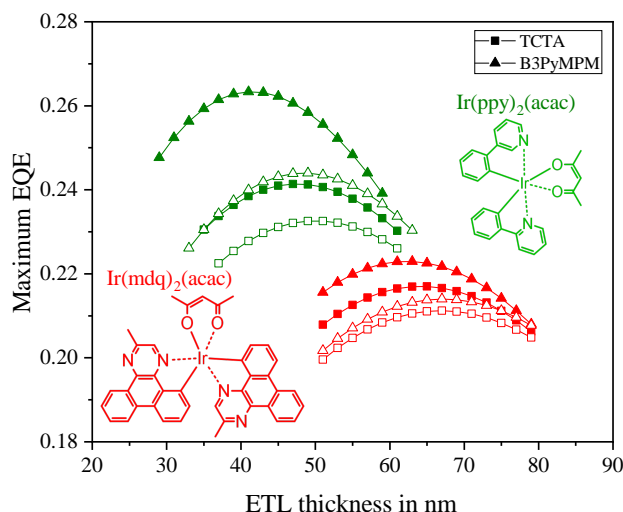
FIG. 2. Maximum possible EQE of the device structures in dependence of electron transport layer thickness. Open symbols are calculated with the average refractive index of the anisotropic materials in the stack.

for $Ir(ppy)_2(acac)$ than for $Ir(mdq)_2(acac)$, but due to differing device structures for the two emitters, this cannot directly be attributed to the different quantum efficiencies. Device structure (3) containing B3PyMPM and $Ir(ppy)_2(acac)$ shows the largest possible EQE in comparison with the other calculations. This can be traced back to the lower refractive index of the organic materials in the stack. Especially TAPC has relatively low optical constants as compared to NPB as hole transport layer (see figure 1), which is directly related to a higher outcoupling efficiency[23]. In the work of Kim *et. al.*[12] a highly efficient device containing B3PyMPM as electron conductor is presented. The extraordinary EQE value of 30.2 % was measured for a device containing 70 nm of ITO, 80 nm of TAPC, 10 nm of TCTA, 30 nm emitting layer and 40 nm electron conductor. The simulation of this device structure (not shown) with anisotropic optical constants as well as an average refractive index yields maximum EQEs of 30.5 % and 27.8 %, respectively. Without horizontal orientation and the resulting birefringence in the transport layer, the devices could thus not exceed the EQE of 30 %. This clearly shows that making use of anisotropic materials is a potential strategy to increase the device efficiency. In the following we will present a strategy to enable electron transport in the hole conductor TCTA in order to exploit benefits from its optical constants.

Due to its high LUMO energy ($-1.6\,eV$[24]) and the low electron mobility[14] TCTA is not favorable for electron transport. As an example, a direct implementation of device structure

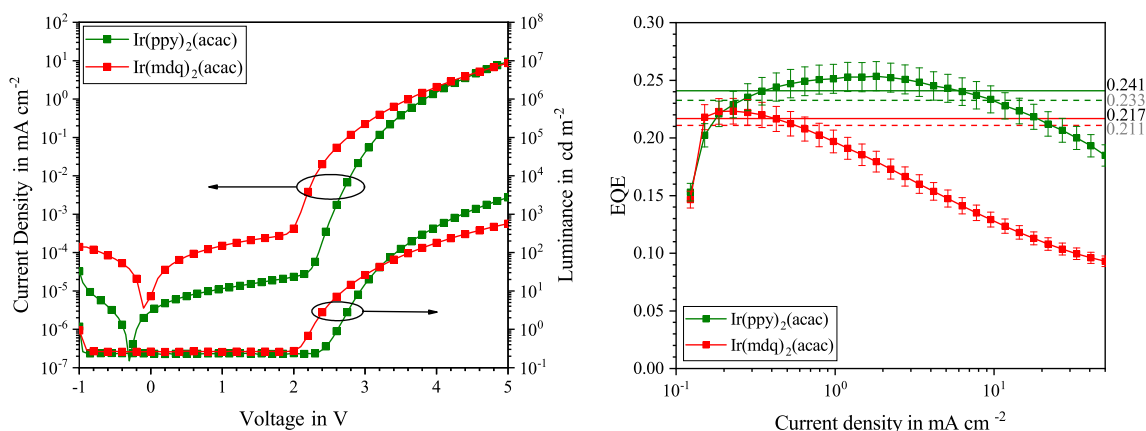FIG. 3. Experimental results for the emitters $Ir(mdq)_2(acac)$ (red) and $Ir(ppy)_2(acac)$ (green) with Cs_2CO_3-doped TCTA as electron transporting layers.

(1) with pure TCTA showed electroluminescence at more than $20\,V$. Thus, it becomes clear that its transport properties have to be modified in order to realize an efficient device employing TCTA as electron conductor. The material cesium carbonate (Cs_2CO_3) was used as an effective n-type dopant in organic electron transport films[25]. Incorporation of the dopant leads to a reduced resistance and injection barrier for the transporting layer[26]. A significant increase of electron injection and transport as well as a higher luminance efficiency has been observed for multiple devices[26–28]. For these reasons we doped the hole conductor TCTA at a concentration of about $c = 5\,\%_{vol}$ with Cs_2CO_3 to enable the electron transport in this layer. For simplicity, we assume that the low amount of dopant does not affect the refractive index of the material in the visible range. Experimental results for the device structures (1) and (2) are shown in figure 3.

In device (1) with the red emitter, the thickness of TCTA was set to $65\,nm$ with a $40\,nm$ thick hole transport layer of NPB. In device structure (2) with the green emitter, the hole and the electron transport layer were fixed at 10 and $50\,nm$, respectively. The red emitting device containing Cs_2CO_3-doped TCTA for electron conduction shows luminescence at a voltage of about $2.1\,V$. This driving voltage is comparable to values achieved with typical electron transport materials[21,29,30]. The doping thus enables electron injection and transport in the material. The OLED reaches a maximum EQE of $22.3 \pm 1.1\,\%$, which is in good agreement with the theoretically predicted value of $21.7\,\%$. This indicates that at the

7

respective operation conditions, electrical losses are negligible. At higher current densities the devices exhibit a rapid roll-off in EQE. This is either a sign of an unbalanced charge carrier injection or a reduced effective radiative quantum efficiency resulting from exciton quenching processes[21].

The green diode containing doped TCTA as electron transporting layer shows a turn-on voltage of about $2.4\,\mathrm{V}$ and an EQE of $25.3 \pm 1.3\,\%$. This again indicates that effective electron transport is enabled by doping with Cs_2CO_3 and the value of the EQE agrees well with the theoretically predicted maximum of $24.1\,\%$. It is noteworthy that the efficiency roll-off is much less pronounced for the green emitting diode compared with its red counterpart. This either indicates that the charge carrier balance is restored for a greater range of current densities or that quenching plays a less significant role for the device containing $Ir(ppy)_2(acac)$. The fact that the triplet lifetime of the green emitter $(0.74\,\mathrm{\mu s})$ is shorter than the value for $Ir(mdq)_2(acac)$ $(1.37\,\mathrm{\mu s}$[20]$)$ argues for a reduced probability for quenching in the device containing $Ir(ppy)_2(acac)$. In the work of Wehrmeister *et. al.*[21] triplet-polaron quenching was identified as the main loss process for the red emitter. As this emitter is directly doped in the hole conductor NPB the device probably exhibits a very good hole injection in the emission layer. On the contrary electrons have to overcome multiple material interfaces before they reach the recombination zone. For these reasons we expect an accumulation of holes at the interface between the emission layer and the hole blocker OXD-7 and a narrow recombination zone at the same interface. In this region a high concentration of free charges and excitons leads to strong non-radiative quenching and a fast roll-off in EQE. In the diode containing $Ir(ppy)_2(acac)$ the situation is different as both, electrons and holes, are injected into the emission layer from different transport layers. Therefore we expect a wider recombination zone with a lower concentration of excitons and free charges. As a consequence less quenching and a slower roll-off in EQE is observed for this device.

In order to quantify the benefit caused by the birefringence of TCTA we calculated the maximum possible EQE assuming the average refractive index of the material. The results for the two different emitters are shown as dashed lines in figure 3. If the birefringence of the electron transport layer is neglected, the simulated maximum EQEs ($21.1\,\%$ for the red diode and $23.3\,\%$ for the green diode) are slightly out of the limits of the measurement accuracy for the achieved efficiencies $22.3 \pm 1.1\,\%$ and $25.3 \pm 1.3\,\%$, respectively. This argues for a benefit of the devices from the anisotropic layers. But the effect is still rather small as

the maximum efficiencies are only changed about 3% in both cases.

In summary we calculated the potential benefit for the negatively birefringent materials B3PyMPM and TCTA as electron transporters in a realistic stack. The maximum EQE is slightly larger if birefringent optical constants are used as compared to isotropic ones. Further we managed to enable electron transport in the hole conductor TCTA by doping with Cs_2CO_3. In combination with a hole blocking layer made from OXD-7 two highly efficient devices with the emitters $Ir(mdq)_2(acac)$ and $Ir(ppy)_2(acac)$ were fabricated. Their efficiency even slightly exceeds the value predicted for isotropic optical constants. This argues for a benefit caused by the birefringence of the material.

REFERENCES

[1]S. Reineke, F. Lindner, G. Schwartz, N. Seidler, K. Walzer, B. Lüssem, and K. Leo, Nature **459**, 234 (2009).

[2]T.-H. Han, Y. Lee, M.-R. Choi, S.-H. Woo, S.-H. Bae, B. H. Hong, J.-H. Ahn, and T.-W. Lee, Nature Photonics **6**, 105 (2012).

[3]W. Brütting, J. Frischeisen, T. D. Schmidt, B. J. Scholz, and C. Mayr, physica status solidi (a) **210**, 44 (2013).

[4]J. Frischeisen, D. Yokoyama, A. Endo, C. Adachi, and W. Brütting, Organic Electronics **12**, 809 (2011).

[5]M. Flämmich, J. Frischeisen, D. S. Setz, D. Michaelis, B. C. Krummacher, T. D. Schmidt, W. Brütting, and N. Danz, Organic Electronics **12**, 1663 (2011).

[6]T. D. Schmidt, T. Lampe, D. Sylvinson M. R., P. I. Djurovich, M. E. Thompson, and W. Brütting, Phys. Rev. Applied **8**, 681 (2017).

[7]D. Yokoyama, A. Sakaguchi, M. Suzuki, and C. Adachi, Applied Physics Letters **93**, 173302 (2008).

[8]D. Yokoyama, Journal of Materials Chemistry **21**, 19187 (2011).

[9]M. K. Callens, D. Yokoyama, and K. Neyts, Optics express **23**, 21128 (2015).

[10]T. Tsutsui, E. Aminaka, C. P. Lin, and D.-U. Kim, Philosophical Transactions of the Royal Society A: Mathematical, Physical and Engineering Sciences **355**, 801 (1997).

[11]D. Yokoyama, H. Sasabe, Y. Furukawa, C. Adachi, and J. Kido, Advanced Functional Materials **21**, 1375 (2011).

[12]S.-Y. Kim, W.-I. Jeong, C. Mayr, Y.-S. Park, K.-H. Kim, J.-H. Lee, C.-K. Moon, W. Brütting, and J.-J. Kim, Advanced Functional Materials **23**, 3896 (2013).

[13]Q. Zhang, B. Li, S. Huang, H. Nomura, H. Tanaka, and C. Adachi, Nature Photonics **8**, 326 (2014).

[14]C. Xiang, W. Koo, F. So, H. Sasabe, and J. Kido, Light: Science & Applications **2**, e74 (2013).

[15]J. Chen, C. Shi, Q. Fu, F. Zhao, Y. Hu, Y. Feng, and D. Ma, Journal of Materials Chemistry **22**, 5164 (2012).

[16]W.-Y. Hung, G.-M. Tu, S.-W. Chen, and Y. Chi, Journal of Materials Chemistry **22**, 5410 (2012).

[17]Y.-Y. Lyu, J. Kwak, W. S. Jeon, Y. Byun, H. S. Lee, D. Kim, C. Lee, and K. Char, Advanced Functional Materials **19**, 420 (2009).

[18]H.-H. Chou and C.-H. Cheng, Advanced materials (Deerfield Beach, Fla.) **22**, 2468 (2010).

[19]R. Meerheim, M. Furno, S. Hofmann, B. Lüssem, and K. Leo, Applied Physics Letters **97**, 253305 (2010).

[20]T. D. Schmidt, D. S. Setz, M. Flämmich, J. Frischeisen, D. Michaelis, B. C. Krummacher, N. Danz, and W. Brütting, Applied Physics Letters **99**, 163302 (2011).

[21]S. Wehrmeister, L. Jäger, T. Wehlus, A. F. Rausch, T. C. G. Reusch, T. D. Schmidt, and W. Brütting, Physical Review Applied **3** (2015), 10.1103/PhysRevApplied.3.024008.

[22]P. Liehm, C. Murawski, M. Furno, B. Lüssem, K. Leo, and M. C. Gather, Applied Physics Letters **101**, 253304 (2012).

[23]N. C. Greenham, R. H. Friend, and D. D. C. Bradley, Advanced Materials **6**, 491 (1994).

[24]H. Yoshida and K. Yoshizaki, Organic Electronics **20**, 24 (2015).

[25]Y. Cai, H. X. Wei, J. Li, Q. Y. Bao, X. Zhao, S. T. Lee, Y. Q. Li, and J. X. Tang, Applied Physics Letters **98**, 113304 (2011).

[26]J. Zhao, Y. Cai, J.-P. Yang, H.-X. Wei, Y.-H. Deng, Y.-Q. Li, S.-T. Lee, and J.-X. Tang, Applied Physics Letters **101**, 193303 (2012).

[27]Y. Li, D.-Q. Zhang, L. Duan, R. Zhang, L.-D. Wang, and Y. Qiu, Applied Physics Letters

90, 012119 (2007).

[28]S.-Y. Chen, T.-Y. Chu, J.-F. Chen, C.-Y. Su, and C. H. Chen, Applied Physics Letters **89**, 053518 (2006).

[29]R. Meerheim, S. Scholz, S. Olthof, G. Schwartz, S. Reineke, K. Walzer, and K. Leo, Journal of Applied Physics **104**, 014510 (2008).

[30]C. Murawski, P. Liehm, K. Leo, and M. C. Gather, Advanced Functional Materials **24**, 1117 (2014).